2D Ultrasonic Flow Mapping of the Secondary Flow Field in Free-Surface Vortices

Sean Mulligan[1], Richard Sherlock[2], John Casserly[3], Giovanni De Cesare[4]

[1] College of Engineering and Informatics, National University of Ireland, Galway, University Road, Galway, Ireland
[2] School of Science, Institute of Technology, Sligo, Sligo, Ireland
[3] Department of Civil Engineering and Construction, Institute of Technology, Sligo, Sligo, Ireland
[4] Laboratory of Hydraulic Constructions (LCH), Ecole Polytechnique Fédérale de Lausanne (EPFL), CH-1015, Lausanne, Switzerland

In this study, an application of two dimensional ultrasonic doppler flow mapping was undertaken on a strong full air core free-surface vortex. The vortex was generated in a scroll type vortex chamber with a subcritical approach flow which have common application in hydraulic structures such as sewer vortex dropshafts and energy dissipaters. A 2D array of ultrasonic Doppler profilers was arranged on the vortex chamber using 7 vertical and 7 horizontally arranged transducers to generate 2D flow maps of the secondary flow field to capture the radial and axial velocity fields. The transducers were multiplexed in a diagonal fashion to generate quasi-instantaneous flow maps of the secondary flow. The 2D velocity fields were smoothed using kriging interpolation and post processed using ParaView. The results highlight interesting cellular structures which develop in the secondary flow along with other global features. These observations have strong implications to improve an understanding of free-surface vortex mechanics and stability.

Keywords: Free-surface vortex, vortex dropshafts, UDP array, vector maps, Taylor-Couette flows

1. Introduction

The re-emerging field of hydraulic structure engineering is in full swing due to existing infrastructure upgrade requirements and the development of innovative hydraulic structures [1]. With this, the hydraulics laboratory environment is being continuously challenged to integrate novel experimental methods to aid in a deeper understanding of flow behaviour within such systems [1]. In this article, we present the application of ultrasonic Doppler profiling in vortex drop shaft chambers which are being increasingly deployed in several hydraulic applications [2]. As will be discussed, free-surface vortex flows exhibit quite complex flow behaviour with regards to turbulence and instability mechanisms which can only be resolvable using advanced measurement techniques [3].

Vortex dropshafts are hydraulic structures which utilize the principles of vortex motion to safely drop water flows through significant height differences thus rendering them applicable in sewer systems or hydropower energy dissipation applications. The free-surface vortex flow is generated in a vortex chamber where the flow enters tangentially and discharges axially through the base of the system [4]. Upon discharge into the dropshaft, the residual centrifugal motion causes the fluid to attach to the shaft walls on its course to the bottom of the shaft where the energy is dissipated through friction along the walls.

One of the main indicators which reflects good performance is the stability of the vortex structure. However, vortex flows contain many complex flow features in the secondary flow field which can trigger often severe turbulence and instability in the main vortex core structure [5]. Characterised by the circulation number N_Γ, the vortex strength and stability are dependent on the ratio of the primary tangential (rotating) velocity v_θ field to the secondary radial v_r and axial velocity v_z field [4]; where the latter induces instability in the flow. Many studies have been undertaken on the general hydraulics of the free-surface vortex and vortex dropshaft structures as is summarised in [4] with minimal studies undertaken on the composition of the secondary flow field [3].

Recently, the technique of ultrasonic Doppler profiling [6] was undertaken on the flow in the subcritical vortex chamber by the current authors [5]. In this interesting study, the authors discovered similarities between the secondary flow field in the turbulent free-surface vortex and the classic Taylor-Couette flow [7] through the existence of cellular structures termed Taylor-like vortices. The structures were quantified using the ultrasonic Doppler profiling (UDP) technique amongst other methods such as analytical modelling, laser induced fluorescence observation and numerical modelling. In this article, the UDP program that was undertaken will be discussed in detail. In the study, the authors developed an application of UDP for vortex chamber flows in order to gain independent radial and axial velocity profiles together with flow maps of the aforementioned secondary flow field using a 2D array of ultrasonic Doppler profilers.

2. Testing Configuration

2.1 Physical Model Test Rig

The physical model employed in the experimental study was constructed from 6 mm transparent acrylic and had an orifice diameter of $d = 0.067$ m, inlet width of $b = 0.067$ m and an inlet radius of $r_{in} = 0.207$ m. The walls scrolled inwards according to the logarithmic spiral. The test geometries were mounted in a 0.85×0.95 m tank

which was 0.5 m deep as highlighted in Figure 1, 4 and 5. The tank contained a centrally positioned 0.1 m orifice and rested on a platform over the storage reservoir. A 0.15 m high chamber was used to allow a void underneath the model to give ample space for UDP transducers on the underside of the chamber.

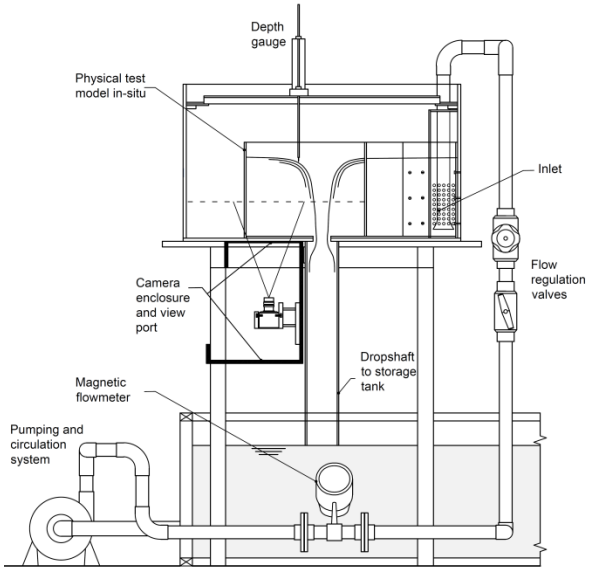

Figure 1: Cross sectional schematic of the vortex flow test rig highlighting the position of the vortex chamber and ancillary hydraulics apparatus.

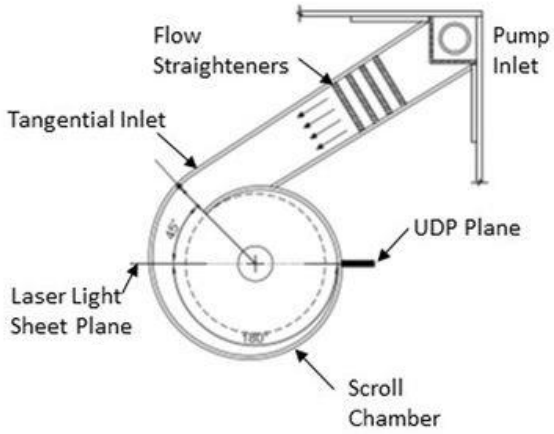

Figure 2: Plan view of the vortex chamber highlighting the inlet, flow straightening plates, laser light sheet plane used in earlier experiments and the UDP plane.

The inlet to the test models comprised a 0.065 m pipe entrance, 0.14 m perforated plates which homogenised the incoming velocity profile. Water was circulated through the system using a centrifugal pump (flow rate of 0 to 3.5 l/s) and was monitored using a magnetic flow meter and regulated using valves. The system delivered a monitoring resolution corresponding to maximum error bars for intake Froude and radial Reynolds numbers of $\mathrm{Fd} = v_z/\sqrt{gd} = \pm 0.019$ and $\mathrm{Rr} = Q/hr = \pm 34$, respectively. Approach flow depths h were expressed as a ratio of the constant orifice diameter $d = 67$ mm by h/d. Tests were performed for 6 approach flow depths corresponding to $h/d = 0.5,\ 1.0,\ 1.5,\ 2.0,\ 2.5$ and 3.0. This resulted in an experimental range of vortex Reynolds number $\mathrm{Re_\Gamma} = 1.38 \times 10^5$ to 2.07×10^5 and circulation numbers $\mathrm{N_\Gamma} = 5.8$ to 31.0. Further details on the hydraulic test rig can be found in [8].

2.2 Ultrasonic Doppler Profiling

The ultrasound Doppler velocity profile method (UDP method) was applied to analyse the secondary flow field in the free-surface vortex. The UDP principle utilises both echography and the Doppler effect to determine the position and velocity of a particle along an ultrasonic beam profile and is described in detail by Takeda [6],[9]. In this application, two-dimensional (2D) flow mapping was implemented by establishing a 7×7 array of ultrasonic transducers along the $r - z$ plane of the vortex to ascertain 2D velocity vectors [10]. The UDP system was supplied by MetFlow SA (Lausanne, Switzerland). Vertical transducers placed at 25 mm centres along the horizontal (r −axis) measured the axial velocity profiles and horizontal transducers spaced at 22 mm along the vertical (z–axis) as highlighted in Figure 3, 4 and 5. The array of transducers were carefully positioned to ensure that the plane was perpendicular to the primary flow field.

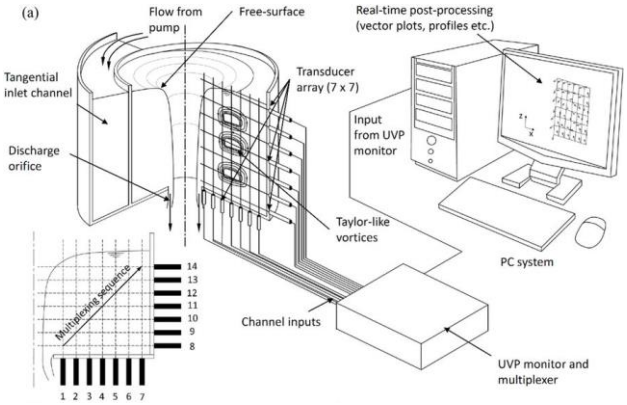

Figure 3: 3D schematic overview of the UDP flow mapping configuration highlighting the transducer array and multiplexing sequence.

A transmitting frequency of 4 MHz was used together with 4 cycles per pulse resulting in a minimum measurable channel width of 0.74 mm. The distance between channels was 0.74 mm. A pulse repetition frequency of 3.52 kHz was used resulting in an in-axis velocity resolution of 2.55 mm/s. 10 micron hollow glass spheres were used for seeding and the number of repetitions $N_{rep} = 32$ was used resulting in a time resolution of 9 ms. The transducers were multiplexed in a diagonal fashion using the following trigger sequence with reference to Fig. 3 (S_t = 1–8, 2–9, 3–10, 4–11, 5–12, 6–13, 7–14). 40 flow maps were obtained for each test over a duration of 224 seconds. The 2D velocity fields were smoothed using kriging interpolation and post processed using ParaView.

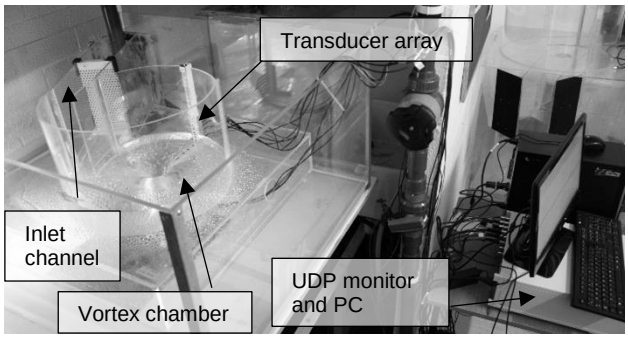

Figure 4: 3D schematic overview of the UDP flow mapping configuration highlighting the transducer array and multiplexing sequence.

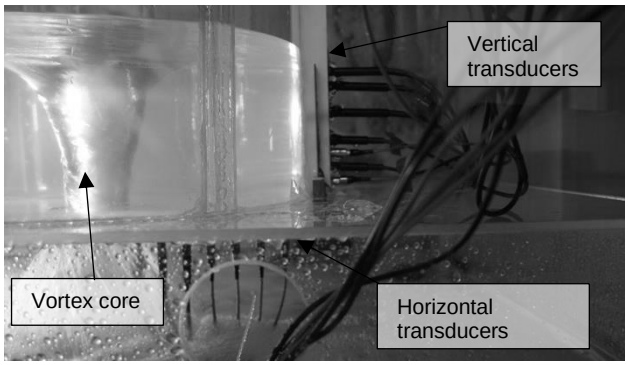

Figure 5: 3D schematic overview of the UDP flow mapping configuration highlighting the transducer array and multiplexing sequence.

3. Results

3.2 Radial and Axial Velocity Profiles

Figure 6 and 7 presents the instantaneous radial and axial velocity profiles for Transducer 8 (T8) and Transducer 4 (T4) respectively (see Figure 3). In the radial case, it can be seen that there was a switch between a positive velocity near the periphery of the chamber and a negative velocity near the outlet. This indicated that a separation point was forming at some region in the radial flow field.

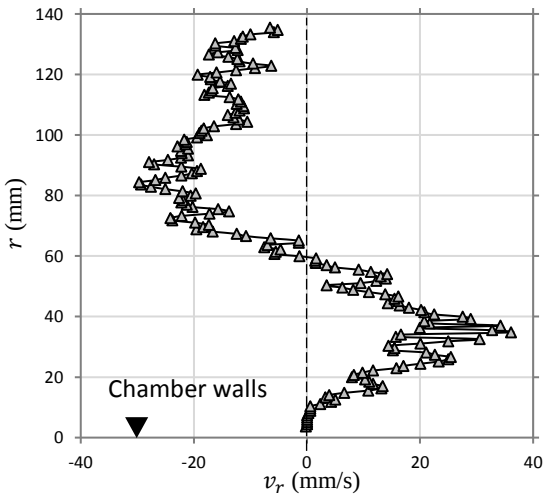

Figure 6: Radial velocity profile at transducers T8

In the axial case, T4 which is positioned close to this separation point highlighted that the velocity switches between positive and negative values at multiple positions throughout the vertical extent of the vortex chamber. Other velocity profiles (not shown here) identified that the axial velocity is in a strong upward direction near the periphery of the chamber.

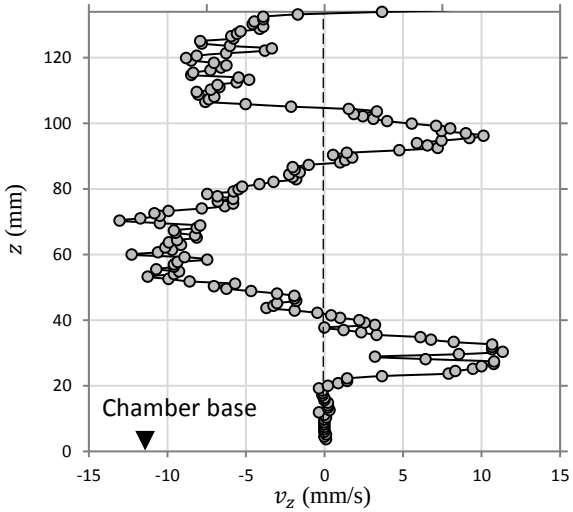

Figure 7: Axial velocity profile at transducers T4

3.3 Spatiotemporal Flow Map

Figure 8 presents a spatiotemporal map of the axial velocity profile over 0.3 seconds time period. The flow map indicates that the profile does not vary significantly within the time frame as indicated by the approximate positive and negative bands determined along the transducer 4 profile. The standard deviation of the axial velocity is also presented using data from 16 profiles.

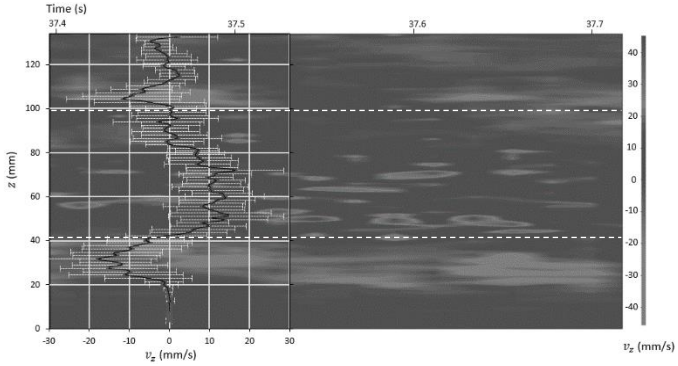

Figure 8: Axial velocity profile at transducers T4

3.4 Secondary Flow Field Vector Maps

Figure 9 (a) and 9 (b) presents the velocity vector maps generated for $Q = 0.635$ l/s and $Q = 1.1$ l/s respectively. Each vector map presents the global flow pattern across the secondary flow field. In each case, the 2D flow maps confirmed the existence of cellular vortices where loosely structured counter rotating vortex cells can be observed.

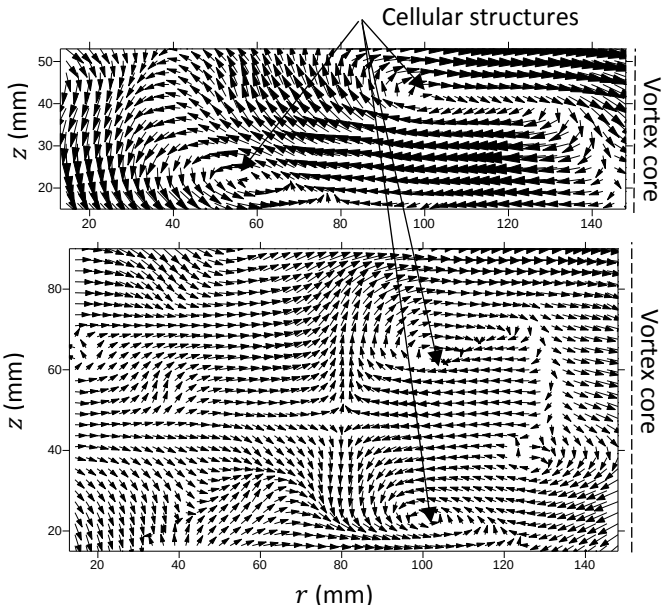

Figure 9: Velocity vector maps generated for (a) $h/d = 1.0$, $Q = 0.635$ l/s and (b) $h/d = 1.5$, $Q = 1.1$ l/s

4. Discussion

As discussed previously, using the horizontal and vertical transducers it was possible to isolate certain regions of the flow to consider instantaneous radial and axial velocities and flow patterns. For the purpose of the previous study carried out by the authors [5], the main aim of the UDP method was to identify signs of cellular flow structures which are recognisable through abrupt changes in the axial velocity field manifesting as a change from a negative velocity to a positive velocity. The change in the sign of the axial velocity is attributed to the UDP beam passing through the edge of a vortex cell. These cellular flow signatures were further substantiated in the generation of the 2D secondary flow field vector maps which also highlighted the structures.

The significance of these findings was that the free-surface vortex flow field, comparable in many ways to the classic Taylor-Couette flow, also exhibited similar instability mechanisms through the presence of Taylor-like vortices. The Taylor-like vortices form due to the presence of a centrifugal driving force which can develop for wall bounded vortex flows. It is pondered that such cellular structures are responsible for producing highly anisotropic turbulence conditions near the core region of a free-surface vortex and may perturb the primary flow field under higher energy conditions causing instability of the free-surface and air core.

Understanding further such flow structures using techniques such as UDP is useful knowledge for applications such as vortex drop shafts where stability of the vortex core is paramount to operation. This study outlines the value of utilising UDP for resolving such complex spatial and temporal flow behaviour.

Conclusions

In this study, an interesting application of the UDP technique was undertaken on a subcritical scroll type vortex chamber which yields application in vortex dropshafts and energy systems. The study highlighted that the UDP technique was valuable in deciphering the complex secondary flow field in a turbulent free-surface vortex comprising axial and radial velocity components which are a function of both space and time. The 7 x 7 array of UDP transducers can resolve a number of instantaneous radial and axial velocities throughout the secondary flow field to identify main global flow features. In addition, signatures for cellular flow structures were identified in the axial velocity profiles which was further substantiated by the velocity vector maps. The cellular flow structures identified were attributed to an unstable centrifugal driving force in the flow and can help explain why free-surface vortices tend to become unstable. Further work is being undertaken by the authors to determine time-series data to resolve turbulence characteristics in the near-field region of the vortex core using the UDP approach and data sets gathered.

References

[1] Hager, W.H. and Boes, R.M., 2014. Hydraulic structures: a positive outlook into the future. Journal of hydraulic research, 52(3), pp.299-310.

[2] Plant, J. and Crawford, D., 2016. Pushing The Limits Of Tangential Vortex Intakes: Is Higher Capacity And Flow Measurement Possible In A Smaller Footprint?. Proceedings of the Water Environment Federation, 2016(12), pp.4108-4136.

[3] Andersen, A., Bohr, T., Stenum, B., Rasmussen, J. J. & Lautrup, B. 2003 Anatomy of a bathtub vortex. Phys. Rev. Lett. 91(10).

[4] Mulligan, S., Casserly, J. & Sherlock, R. 2016. Effects of Geometry on Strong Free-Surface Vortices in Subcritical Approach Flows. J. Hyd. Eng. 142(11)

[5] Mulligan, S., De Cesare, G., Casserly, J. and Sherlock, R., 2018. Understanding turbulent free-surface vortex flows using a Taylor-Couette flow analogy. Scientific reports, 8(1), p.824.

[6] Takeda, Y. 2012. Ultrasonic Doppler velocity profiler for fluid flow. (Vol. 101) (Springer Science & Business Media)

[7] Taylor, G. I. 1923. Stability of a viscous liquid contained between two rotating cylinders. Phil. Trans. Roy. Soc. Lond. Ser. A, Math. Phys. 223, 289–343,

[8] Mulligan, S. 2015. Experimental and numerical analysis of three-dimensional free-surface turbulent vortex flows with strong circulation

[9] Takeda, Y. & Kobayashi, K. 1991. Ultrasonic flow visualization of transient behavior of taylor vortex flow. Exp. Numer. Flow Visual. ASME FED 128, P231–237

[10] Althaus, J.M.J., De Cesare, G. and Schleiss, A.J., 2016. Release of suspension particles from a prismatic tank by multiple jet arrangements. Chemical Engineering Science, 144, pp.153-164.